nature photonics

Article

https://doi.org/10.1038/s41566-023-01266-1

Handwriting of perovskite optoelectronic devices on diverse substrates

Received: 22 September 2022

Accepted: 5 July 2023

Published online: 07 August 2023

Check for updates

Junyi Zhao [1], Li-Wei Lo [1,2], Zhibin Yu [3] ✉ & Chuan Wang [1,2] ✉

Paper and textiles that are commonly used in our daily lives hold great potential as platforms for next-generation flexible and wearable electronics. However, strategies for fabricating light-emitting diodes and photodetectors on different substrates are restricted in terms of their quantity and variety as strict flatness and smoothness are often required. Here we develop a highly versatile, scalable and eco-friendly handwriting approach to draw multicolour perovskite light-emitting diodes and perovskite photodetectors on various substrates, including paper, textiles, plastics, elastomers, rubber and three-dimensional objects. Our method uses common ballpoint pens filled with newly formulated inks of conductive polymers, metal nanowires and multiple perovskites for a wide range of emission colours. Just like writing with multicoloured pens, writing layer-by-layer with these functional inks enables perovskite optoelectronic devices to be realized within minutes. This process can be carried out by individuals without specialized training. The handwritten perovskite light-emitting diodes can exhibit a brightness as high as 15,225 cd m^{-2}, a current efficiency of 6.65 cd A^{-1} and a turn-on voltage of 2.4 V. The perovskite photodetectors exhibit an on/off ratio of over 10,000 and a responsivity of up to 132 mA W^{-1}. This work offers a route to the integration of perovskite optoelectronics in low-cost and large-area application scenarios such as electronic textiles, electronic paper, smart packaging and other disposable electronics and wearables.

Optoelectronic devices (for example, light-emitting diodes (LEDs) and photodetectors (PDs)) have become integral for emerging technologies such as flexible displays[1–3], human–machine interfaces[4,5], biomimetic image sensors[6–8] and wearable electronics[9]. Their mainstream fabrication involves spin coating, vacuum-based evaporation/sputtering and etching[10,11]. Despite offering great reproducibility and device performance, these conventional processes may be time- and energy-consuming, taking hours or days to complete one batch of samples, even before the time for stencil/mask design and manufacture is taken into consideration. For large-area applications and mass production, printing techniques such as blade printing[12], bar coating[13], electrohydrodynamic printing[14] and inkjet printing[15] have been studied widely as alternatives. However, printing methods have limitations, such as tedious alignment/calibration steps and a weak patterning capability on non-planar surfaces. Moreover, ink-wetting requirements limit the substrate selection to rigid and flat glass[11,13,16–19] or planar and smooth thin films[20–22]. The emerging demand for disposable and wearable electronics necessitates the fabrication of devices on ubiquitous substrates. For instance, recent studies have reported optoelectronic devices on paper[23–26] and textiles[27–29]. However, nearly all of these involved either the paper/textile being coated with a polymer for surface planarization[23,26] or the use of artificially synthesized

[1]Department of Electrical & Systems Engineering, Washington University in St. Louis, St. Louis, MO, USA. [2]Institute of Materials Science and Engineering, Washington University in St. Louis, St. Louis, MO, USA. [3]Department of Industrial and Manufacturing Engineering, Florida State University, Tallahassee, FL, USA. ✉e-mail: zyu@fsu.edu; chuanwang@wustl.edu

paper-like membrane/films[24], rather than using unmodified substrates that are easily accessible in daily life.

Regarding optoelectronic semiconductor materials, halide perovskites have drawn substantial interest for their solution processability and exceptional balance of cost and performance. Perovskite materials possess a tunable bandgap, strong photoluminescence (PL) and electroluminescence (EL), and a high absorption coefficient, making them ideal for next-generation light emitters[10,16,30–32] and photosensors[6,18,20]. For example, the perovskite bandgap can be adjusted by substituting the halide element to enable the easy production of multicolour perovskite light-emitting diodes (PeLEDs) with the desired emission wavelengths for displays and lighting applications[11,33]. Various strategies can be used to enhance the device performance, and include lowering the material-level dimensionality from a three-dimensional (3D) perovskite to a quasi-two-dimensional Ruddlesden–Popper perovskite (quasi-2D RPP)[11,17], lowing the structure-level dimensionality from bulk[18,34] to nanowires[6,7] or nanocrystals[3,16,30] and optimizing the crystallization and film morphology through polymer blending[12,35]. Despite the great promise of perovskites, the fabrication of PeLEDs and perovskite photodetectors (PePDs) reported so far has relied predominantly on spin coating and microfabrication.

In this Article we report a versatile handwriting strategy that is literally as straightforward as holding a ballpoint pen in the hand to write on the target substrate, which enables rapid access to functional optoelectronic devices that are 'drawn' on demand, even by untrained individuals, in a time-saving and cost-effective manner. Notably, the process eliminates the restrictions of conventional substrates to provide devices that are built directly on objects that are ubiquitous in daily life, such as paper, textiles, gloves, rubber balloons, plastic films, elastomers and even 3D substrates. The handwriting also enables an ultrafast and eco-friendly fabrication process that is capable of delivering one batch of completed devices within a few minutes. One major challenge does arise from the rough surface morphology and high absorbency of fibrous paper, however, which results in an uneven film thickness and current leakage. To address this issue, poly(ethylene oxide) (PEO) can be blended into poly(3,4-ethylenedioxythiophene) poly(styrene sulfonate) (PEDOT:PSS) to adjust the ink viscosity and rheology, ensuring that the composite ink not only works as a bottom electrode but partially soaks into the surface layer of paper to prime and planarize the surface morphology for better drawing and deposition of upper layers. A collection of halide perovskite inks, including $MAPbX_3$ ($MA = CH_3NH_3$; X = Cl, Br, I or their mixtures) and the butylammonium (BA) group-based quasi-2D RPP, was synthesized to achieve emission wavelengths covering the entire visible spectrum. We have demonstrated that perovskite optoelectronic devices, including multicolour PeLEDs, vertical photodiodes and lateral photoconductors, can be manufactured in an ambient environment using just ballpoint pens. This technology offers a promising route to emerging applications in low-cost customizable electronic textiles (e-textiles), electronic paper (e-paper), smart packaging and wearable electronics.

Handwriting of PeLEDs on diverse substrates

The process of handwriting perovskite optoelectronic devices in either a vertical or a lateral device configuration is schematically illustrated in Fig. 1a. The process is widely applicable, and the ink deposition follows our everyday handwriting habits, progressing in a layer-by-layer manner from bottom to top. Taking the $MAPbBr_3$ PeLED as an example, the as-prepared functional inks were loaded into pre-cleaned ballpoint pens (Fig. 1b, bottom (left and right) and Methods) and written on the paper substrate in sequence (Fig. 1b, top). A close-up view shows the PEDOT:PSS electrode being drawn in a controlled manner when the ballpoint pen is brought into contact with the paper (Fig. 1b, middle). The scanning electron microscope (SEM) image of a hand-drawn PeLED on paper shows the multilayer structure formed on the percolating cellulose fibres (Fig. 1c). The handwritten PeLED on paper exhibited great brightness and flexibility (Fig. 1d). Furthermore, by substituting the halide elements in the perovskite and formulating inks with various halide element compositions, multicolour emitters spanning the entire visible spectrum are obtained. The measured PL spectra and corresponding fluorescent photographs are presented in Fig. 1e. Using multiple perovskite inks, a handwritten logo on aluminium foil was demonstrated (Fig. 1f, top), and red, green and blue multicolour luminous emissions can be observed under ultraviolet (UV) illumination (Fig. 1f, bottom). In addition, the showcased paper displays demonstrate the EL of the PeLEDs with various colours and shapes (Fig. 1g,h).

In terms of substrates, glass is used widely for perovskite optoelectronics due to its transparency, stability and microfabrication compatibility. However, the all-solution handwriting approach enables the fabrication of devices under ambient conditions on materials that cannot withstand high temperature such as plastics or rubber, and even on everyday materials such as paper and textiles. For example, Fig. 2a demonstrates a luminous PeLED drawn on the fingertip of a vinyl glove that can tolerate excessive deformation from repeated fist grasping and releasing. For depositing materials on complex and 3D geometries, handwriting outperforms printing since the roll-to-roll printing method struggles with uniform patterning on multidimensional surfaces and the jetting components cannot reach the interior surfaces. To demonstrate the unique strength of the handwriting approach, a PeLED was patterned on the interior sidewall of a glass vial (Fig. 2b) in a straightforward handwriting manner (Supplementary Fig. 1). A PeLED handwritten on the spherical surface of a rubber balloon survived tens of inflation–deflation cycles with a biaxial stretch of over 40% (corresponding to an area increase of 96%), thus revealing its sufficient mechanical stretchability (Fig. 2c and Supplementary Fig. 2). PeLEDs handwritten on plastic films exhibited remarkable flexibility and durability, as shown by a 180°-folded lit-up PeLED strip on the edge of a sharp blade (Fig. 2d), without any noticeable damage. Such on-demand and rapid fabrication, complemented by an exceptional device performance, could further enable many interesting applications and creations. For instance, a low-cost 'light-emitting paper' device was demonstrated by handwriting a green PeLED directly onto the reverse side of printing paper with a cartoon traffic-light graphic printed on the front side (Fig. 2e). When powered using a 3.6 V coin-cell battery, the PeLED could be switched on/off to simulate the traffic-light operation. Finally, e-textiles are regarded as a promising platform for next-generation flexible displays and wearable electronics[27,29]. However, the challenge here lies in the difficulty of fabricating deformable and high-performance optoelectronic devices on porous textiles (Fig. 2f and Supplementary Fig. 3). Handwriting can serve as a facile approach for obtaining functional PeLEDs on textiles that include cotton (Fig. 2g) and various woven forms of polyester (Fig. 2h–j). Moreover, to showcase the practical applicability of PeLEDs in e-textiles, both the size scalability and colour tunability are demonstrated by drawing PeLEDs of different shapes (square, rectangle and circle) and colours (green, red and blue) at various sizes, ranging from the micrometre to millimetre scale, on a textile substrate (Fig. 2k). Supplementary Table 1 summarizes the state-of-art fabrication techniques for flexible PeLEDs, and highlights the advantages of the handwriting strategy.

Preparation of paper substrate and bottom electrode

Inspired by a well-known phenomenon in daily life, where a piece of paper smeared with oil will look translucent, an optional pre-treatment step was developed to create a semi-transparent paper substrate for effectively improving the PeLED luminance and efficiency. As shown in Fig. 3a, the oil-treated paper (Fig. 3a(ii)), even after being coated with a PEDOT:PSS film (Fig. 3a(iii)), was more transparent than the pristine paper sample (Fig. 3a(i)). The transmittance of oil-treated paper increased from 24.84% to 70.28% for green light (530 nm), approaching an acceptable level for LED substrates (Supplementary Table 2).

https://doi.org/10.1038/s41566-023-01266-1

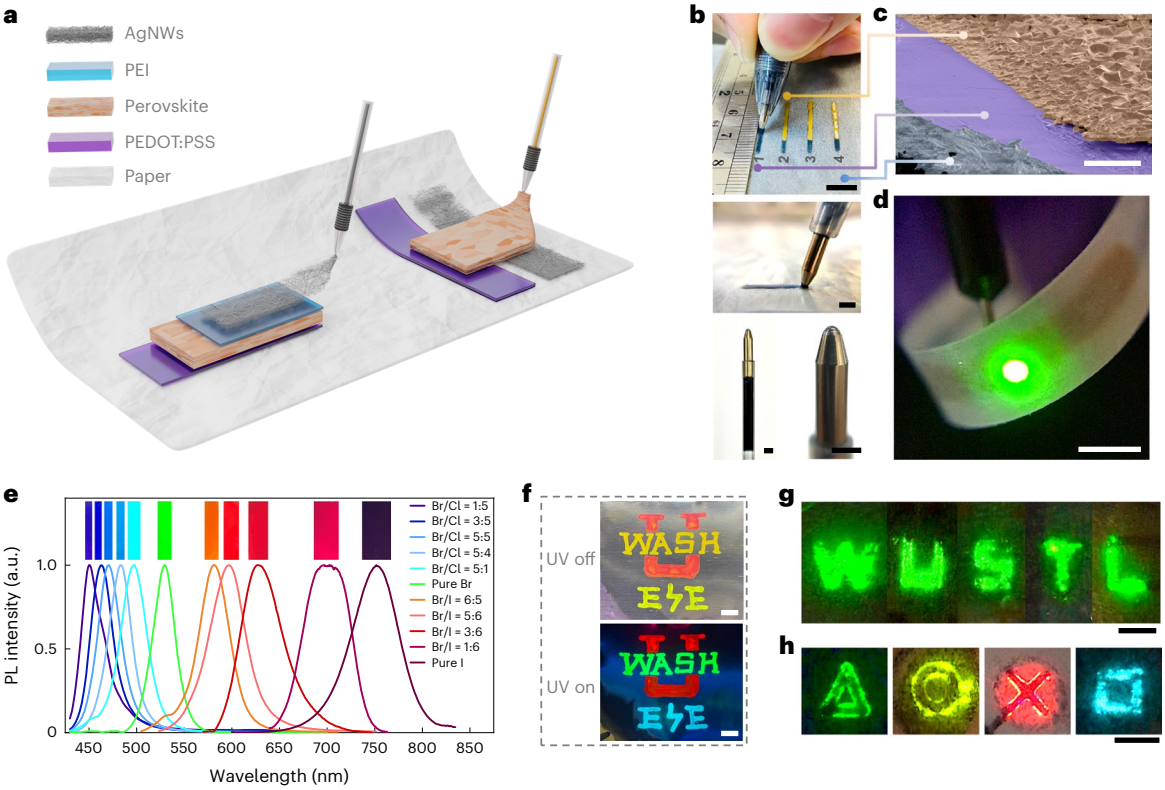

Fig. 1 | Handwriting of perovskite optoelectronic devices with multicolour light emissions. a, Schematic illustration of the universal handwriting approach to fabricate perovskite optoelectronic devices with a vertical (left) or lateral (right) structure. **b**, Top: steps for preparing a PeLED on a paper substrate through layer-by-layer writing using a commercial ballpoint pen, which include (1) writing the PEDOT:PSS bottom electrode, (2) writing the perovskite emissive layer, (3) writing the polyethylenimine (PEI) buffer layer and (4) writing the silver nanowire (AgNW) top electrode. Middle: close-up view of the handwriting process of the PEDOT:PSS bottom electrode. Bottom left and right: expanded views of the as-prepared ballpoint pen loaded with the formulated ink. Scale bars, 1 cm (top) and 2 mm (middle and bottom). **c**, Isometric-view SEM image of a representative handwritten PeLED on a paper substrate. Scale bar, 100 µm. **d**, Image showing the EL emitted from a handwritten PeLED on a piece of untreated pristine printer paper as it is being bent, powered by a 3.6 V coin-cell battery. Scale bar, 5 mm. **e**, Normalized PL spectra with insets showing the corresponding fluorescent photographs taken of $MAPb(Cl_{1-x}/Br_x)_3$, $MAPbBr_3$, $MAPb(Br_x/I_{1-x})_3$ and $MAPbI_3$ thin films. **f**, Photographs showing a multicolour emitter on aluminium foil written using ballpoint pens filled with $MAPbBr_{1.36}I_{1.64}$ (red), $MAPbBr_3$ (green) and $MAPbCl_{1.33}Br_{1.67}$ (blue) inks without (top) and with (bottom) UV light illumination. Scale bars, 500 µm. **g**,**h**, Photographs of the EL from handwritten PeLEDs on a paper substrate displaying the text 'WUSTL' (**g**) and multicolour geometric figures (**h**). Scale bars, 1 mm.

Moreover, an additional polydimethylsiloxane (PDMS) coating created a hydrophobic non-absorbing surface, reducing the adherence of the PEDOT:PSS ink and resulting in more transparent conductive films (Fig. 3a(iv),(v)).

To improve the handwriting experience and patterning resolution, high-molecular-weight PEO was mixed into PEDOT:PSS to modify the ink rheology. The transmittance spectra of the handwritten PEDOT:PSS/PEO composite films on oil-treated paper show that increasing the PEO weight ratio improves transmittance by diluting the PEDOT:PSS ink (Fig. 3b and Supplementary Table 3). The addition of PEO also increases the ink viscosity and contact angle, limiting the spreading of the ink on the paper and aiding in more precise and controllable patterning. The correlation between the feature width and the PEO ratio indicates that a higher PEO ratio narrows the writing path when using the same pen, facilitating the fabrication of smaller devices or denser integrations (Fig. 3c). In practice, the handwriting resolution of the functional PeLEDs could be reduced further to below 200 µm if pens with finer ballpoint tips are used, approaching the resolution limit of inkjet printing on a paper substrate (Supplementary Fig. 4). By contrast, however, resolution improvement comes at the cost of electrical conductivity (Fig. 3d). Considering the tradeoff between transparency, resolution and conductivity, an ink formulation of PEDOT:PSS with 30 wt% PEO was selected, which provides a 63.51% optical transparency, an 852 µm writing linewidth and a minimal sheet resistance of approximately 166 Ω sq^{-1}. The mechanical compliance of the PEDOT:PSS/PEO composite electrodes on paper was tested under various deformation modes that included twisting, bending and folding, and showed less than 3%, 6% and 10% conductivity degradation, respectively, after 5,000 cycles (Fig. 3e). In addition, the PEO additive plays an essential role in enabling direct handwriting on regular non-treated paper substrates by improving film morphology and preventing short circuits. PEO increased the PEDOT:PSS ink viscosity, slowing down ink penetration into deeper substrate layers and filling voids among the percolating cellulous networks. Hence, the PEDOT:PSS/PEO layer acts as both an electrode and a self-planarization film that is anchored securely to the cellulose fibres. Figure 3f illustrates the surface morphology differences between pure PEDOT:PSS and PEDOT:PSS/PEO composite electrodes on paper. The self-planarization effects of the PEDOT:PSS/PEO composite ink are systematically discussed in Supplementary Fig. 5.

Characterization of handwritten multicolour PeLEDs on paper

Depositing pinhole-free perovskite films poses a critical challenge in obtaining high-quality optoelectronic devices, especially in the context of a handwriting approach that involves the manual extraction of ink from pen tips. To overcome this challenge, different host polymers in the perovskite/polymer blends were studied to identify the optimal formulation for achieving appropriate active layers in LEDs and PDs.

https://doi.org/10.1038/s41566-023-01266-1

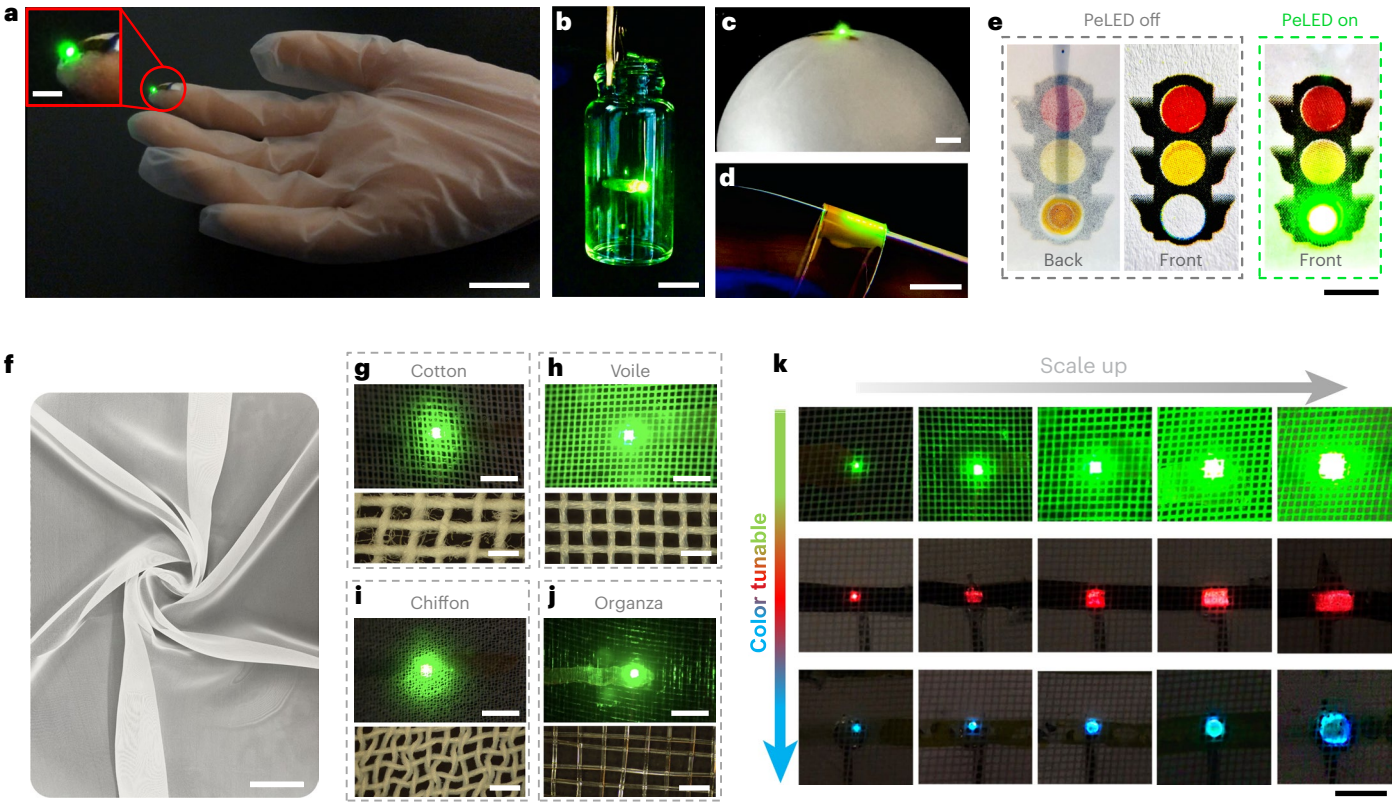

Fig. 2 | Handwritten PeLEDs on ubiquitous objects in daily life. a–**d**, Images showing the EL of PeLEDs drawn on diverse substrates, including a vinyl glove (**a**), the interior sidewall of a glass vial (**b**), a rubber balloon (**c**) and a folded polyethylene terephthalate film (**d**). Scale bars, 2 cm (**a**), 5 mm (inset of **a**), 1 cm (**b**), 1 cm (**c**), 5 mm (**d**). **e**, 'Flashing traffic light' demonstration with a PeLED drawn on the reverse side of untreated pristine printer paper and being switched on and off. Scale bar, 5 mm. **f**, Commercial voile textile purchased as a substrate for the drawing of PeLEDs. Scale bar, 5 cm. **g**–**j**, PeLEDs written on various textiles, including cotton (**g**), voile (**h**), chiffon (**i**) and organza (**j**). Scale bars, 5 mm (top) and 500 µm (bottom). **k**, Size scaling of multicolour PeLEDs patterned on textiles. All EL images were obtained with the PeLED powered using a coin-cell battery. Scale bar, 5 mm.

Composite inks were obtained by dispersing perovskite crystals into a PEO, polystyrene (PS) or poly(methyl methacrylate) (PMMA) polymer matrix. Specifically, the perovskite/PEO composition offers am optimal ink rheology and viscosity for precise and smooth patterning; the perovskite/PS composite improves the uniformity and density of the perovskite crystal arrangement, enhancing the brightness and reducing the leakage current of the PeLEDs; the perovskite/PMMA composition reduces grain defects and boundaries, facilitating the transport of photocarriers in the PDs (Supplementary Fig. 6).

To evaluate the handwritten PeLEDs on pristine paper, reference devices on PDMS-coated paper were also prepared with the same device structure (Fig. 4a–d). The only difference was the selection of substrate. PeLEDs written on pristine paper yielded a slightly rougher morphology, as the PEDOT:PSS/PEO electrode partially penetrated the paper surface. By contrast, the PDMS coating perfectly planarized the paper surface, facilitating the formation of a compact perovskite arrangement and yielding smoother and cleaner interfaces between the different layers. The PEI buffer layer was used to protect the underlying perovskite layer from being eroded by the AgNW ink on top and was also regarded as a work-function modifier to reduce the Schottky barrier, thereby facilitating electron injection[15,36]. Higher-magnification SEM images are presented in Supplementary Fig. 7 to visualize the PEI interfacial layer, which is too thin to be distinguished here.

The performance of the green PeLEDs on pristine paper and PDMS-coated paper substrates were characterized, and included the current density–voltage (*J*–*V*), luminance–voltage (*L*–*V*) and current efficiency–voltage (*CE*–*V*) curves (Fig. 4e,f). The maximum luminance on pristine paper reached 3,980 cd m^{-2} at 6.6 V (Fig. 4e inset), which is lower than the luminance of 11,867 cd m^{-2} at 7.8 V on the PDMS-coated paper, but is still a notable performance considering the simplicity of the handwriting approach. The PeLED on pristine paper had a lower turn-on voltage (2.9 V) compared with the PDMS-coated paper (3.15 V), making it ideal for disposable and low-cost light sources powered by a 3.6 V coin-cell battery while producing over 600 cd m^{-2} of brightness, which is sufficient for most display applications in daily life. The peak *CE* was 1.365 cd A^{-1} and 4.6 cd A^{-1} on pristine paper and PDMS-coated paper, respectively. The impact of the perovskite layer thickness on the PeLED performance was also investigated (Supplementary Fig. 8). The performance variation of the handwritten PeLEDs on multiple substrates indicates that the PeLED written directly onto a PDMS substrate exhibited the best performance with a turn-on voltage of 2.4 V, a luminance of 15,225 cd m^{-2} and a current efficiency of 6.65 cd A^{-1} (Supplementary Fig. 9a–c and Table 4). In addition to the aforementioned multicolour perovskite formulations (Fig. 1e), the BA group was introduced to obtain the $BA_2(MAPbI_3)_{n-1}PbI_4$ quasi-2D RPP (Supplementary Fig. 10), which substantially boosted the brightness and efficiency of red PeLEDs. The *J*–*V*, *L*–*V* and *CE*–*V* curves of red and blue PeLEDs are shown in Fig. 4g,h. The red PeLED on pristine paper exhibited a maximum luminance of 1,213 cd/m^2 at 8.7 V with a turn-on voltage of 3.25 V, while the blue PeLED exhibited a maximum luminance of 516 cd/m^2 at 8.95 V with a turn-on voltage of 3.5 V (Fig. 4g insets). Peak *CE* of the red and blue PeLEDs reached 3.36 cd A^{-1} and 1.16 cd A^{-1}, respectively. The device uniformity statistics and performance metrics for multicolour PeLEDs are presented in Supplementary Fig. 9 and Table 4. The mechanical durability and flexibility of the handwritten PeLEDs were also evaluated. As each layer of the PeLED was designed

https://doi.org/10.1038/s41566-023-01266-1

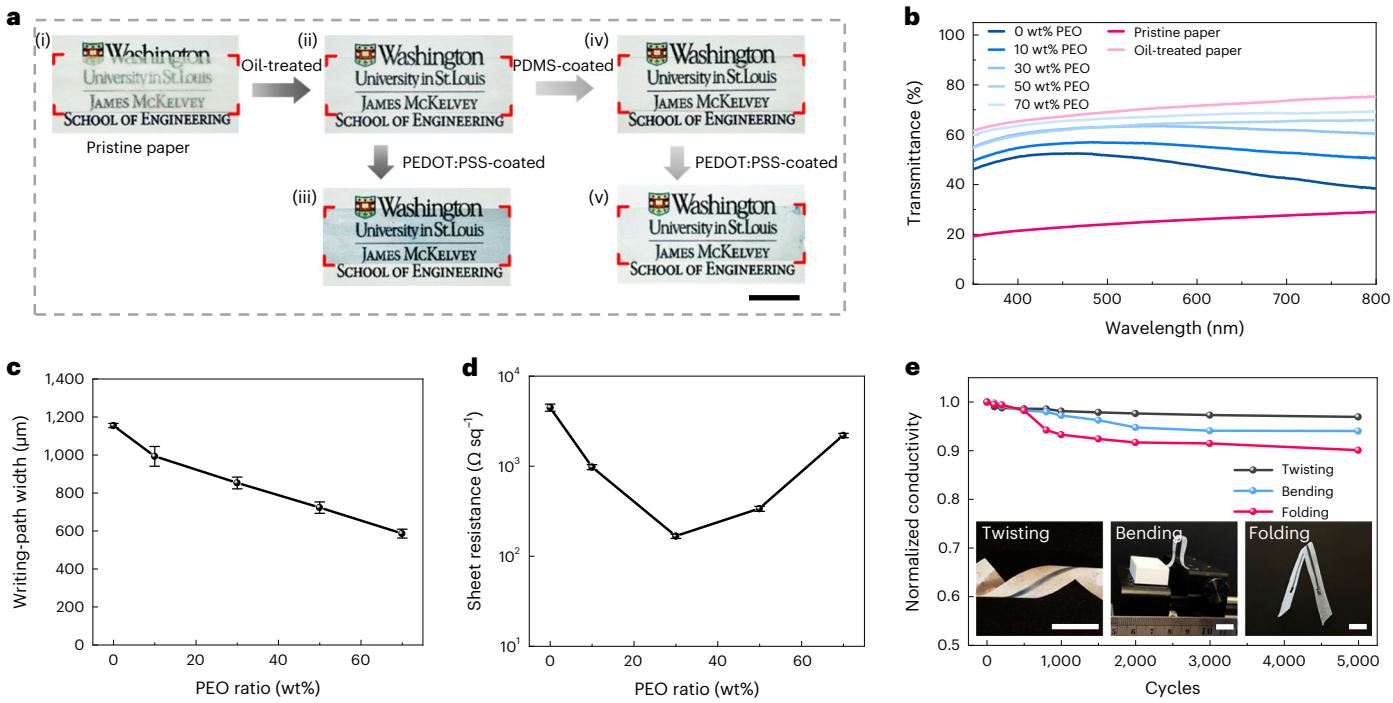

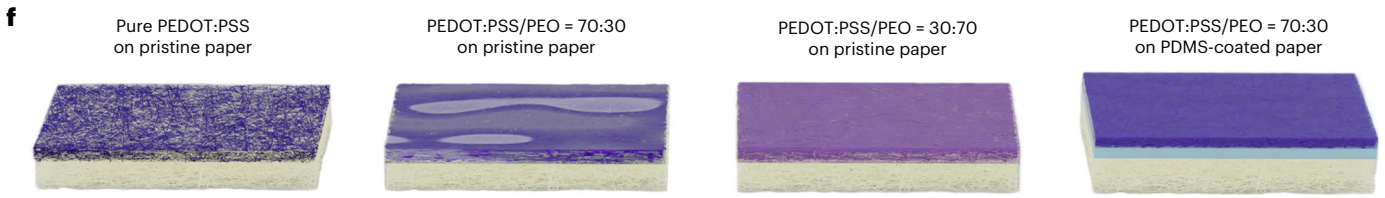

Fig. 3 | Methods for preparing the paper substrate and characterisation of the PEDOT:PSS/PEO bottom electrode. a, Pictures illustrating the use of oil-treatment and PDMS-coating approaches to increase the optical transparency of paper. The region inside the red box shows the treated paper sample placed on another sheet of office paper on which a logo is printed, for better viewing of the sample transparency. Pristine paper (i), oil-treated paper (ii), oil-treated paper with PEDOT:PSS film coating (iii), oil-treated paper with PDMS coating (iv), oil-treated paper with PDMS coating and PEDOT:PSS film coating (v). Scale bar, 1 cm. **b**, Transmittance spectra of handwritten PEDOT:PSS/PEO composite films with different PEO weight ratios on an oil-treated paper substrate. **c**, Path width of the handwritten PEDOT:PSS/PEO composite films as a function of the PEO additive weight ratio. Data are presented as the mean value ± standard deviation from five independent devices. **d**, Sheet resistance of the handwritten PEDOT:PSS/PEO electrode on a paper substrate as a function of the PEO additive weight ratio. Data are presented as the mean value ± standard deviation from five independent devices. **e**, Evaluation of the normalized conductivity of the PEDOT:PSS/PEO composite electrodes, drawn on a paper substrate, after subjecting them to twisting, bending and folding for up to 5,000 cycles. The insets show images of the samples and the representative twisting, bending and folding conditions used in the tests. Scale bars, 1 cm. **f**. Schematics showing that the PEO additive in the PEDOT:PSS/PEO composite ink can help to encapsulate and planarize the percolating cellulose fibres of the pristine paper substrate, resulting in a surface morphology similar to the PDMS-coated paper substrate.

to be intrinsically stretchable, the devices were able to survive severe deformations. The device on paper can be bent to a concave position (with a 1 mm curvature radius) for up to 5,000 cycles, with a drop in the normalized luminance of only ~5% for the green PeLEDs on both the pristine paper and PDMS-coated paper substrates (Fig. 4i). The normalized *CE* decreased by ~5% for the device on PDMS-coated paper but increased by ~6% on pristine paper (Supplementary Fig. 11). Notably, the bending test took tens of hours to complete (Supplementary Fig. 12a), indicating that the handwritten and unencapsulated PeLEDs have a decent lifetime in ambient air for long-term use. The continuous operational stability in air was examined as well, showing decent lifetime (T_{50}) values (that is, the time required for the luminance to drop to 50% of its initial value) of over 70 min for the green PeLEDs, 5.2 min for the red PeLEDs and 3.5 min for the blue PeLEDs (Supplementary Fig. 12b).

Characterization of handwritten PePDs on paper

The handwriting strategy is highly versatile and applicable for the fabrication of other optoelectronic devices, such as PePDs. Two representative PePD configurations, that is, vertical photodiodes and lateral photoconductors, were fabricated on paper and tested. The vertical photodiode (Fig. 5a) consists of a PEDOT:PSS/PEO anode, a $MAPbBr_3$/PMMA photoactive layer and an AgNW cathode; the lateral photoconductor (Fig. 5d) has PEDOT:PSS/PEO and AgNW asymmetric electrodes covered by the $MAPbBr_3$/PMMA capping in the channel. Current–voltage (*I*–*V*) curves were characterized in the dark and under 532 nm illumination at various power densities. The vertical photodiode exhibited a low dark current (I_{dark}) of hundreds of picoamperes and a high light current (I_{light}) of tens of microamperes under illumination at 500 mW cm^{-2}, yielding a PD on/off ratio (I_{light}/I_{dark}) of 1.1×10^4 at −0.5 V bias or 9.2×10^3 at −2.5 V bias (Fig. 5b). Clear diode behaviour with a rectification ratio of over 300 under dark conditions (at −3/+5 V) was observed. The open-circuit voltage (V_{oc}) gradually increased to approximately 1 V with increasing irradiation intensity. Furthermore, the built-in electric field in the photodiode enables a low or even a zero bias voltage to extract photogenerated carriers for the photocurrent. By contrast, the lateral photoconductor exhibited drastically different behaviour with roughly linear and symmetric *I*–*V* characteristics (Fig. 5e). A small short-circuit current (J_{sc}) and a consistent V_{oc} (~0.75 V)

https://doi.org/10.1038/s41566-023-01266-1

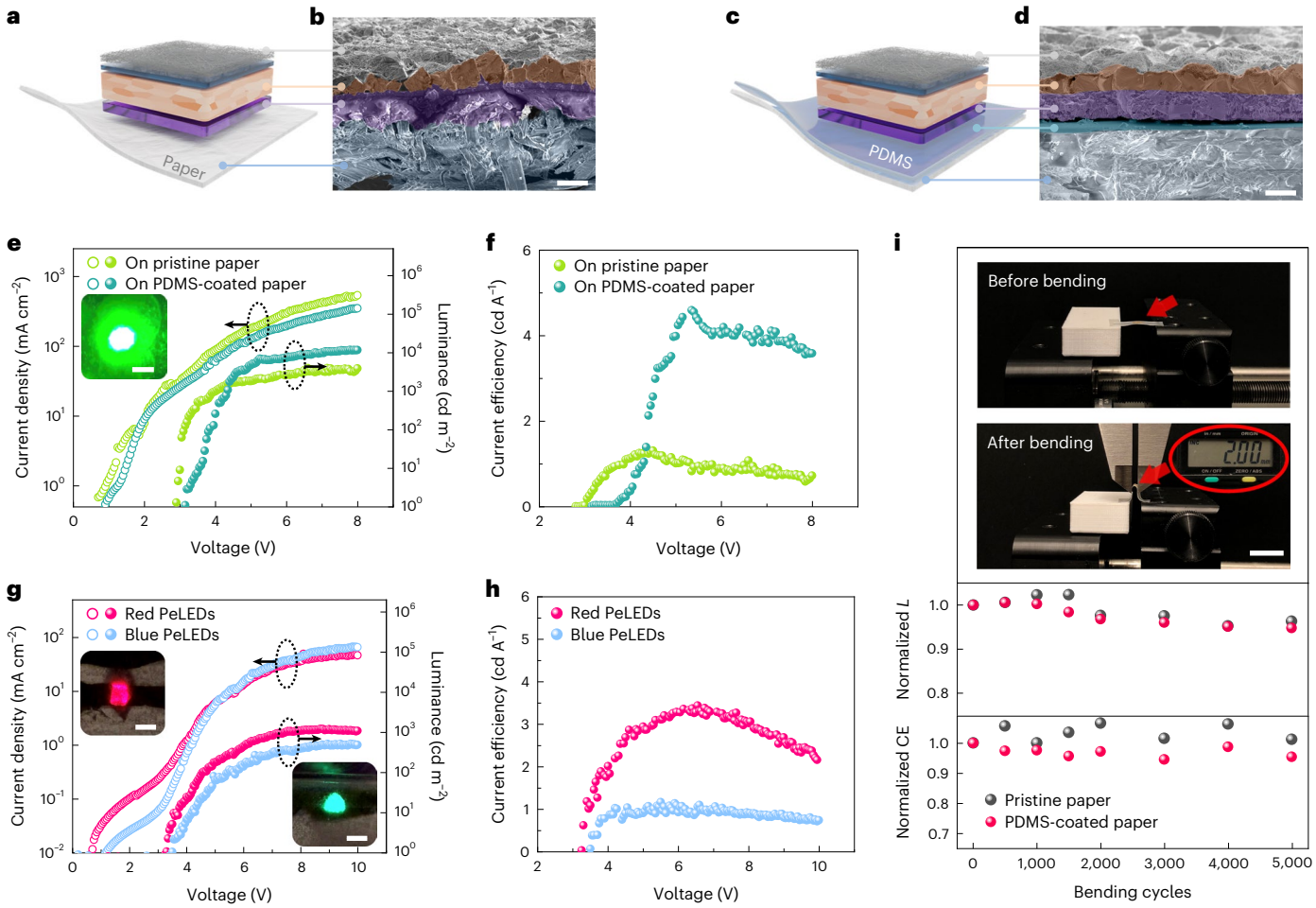

Fig. 4 | Performance characterization of the handwritten multicolour PeLEDs on paper. a–**d**, Schematics of the PeLEDs handwritten on a pristine paper substrate (**a**) and a PDMS-coated paper substrate (**c**), where both have the same device structure of a PEDOT:PSS/PEO anode (purple), a perovskite/PS light-emitting layer (orange), a PEI buffer layer (blue-grey) and a AgNW cathode (grey). The corresponding cross-sectional SEM images of the device (**b**,**d**). Scale bars, 5 µm. **e**,**f**, Characterization of the current density–voltage (*J*–*V*) and luminance–voltage (*L*–*V*) curves (**e**) and the current efficiency–voltage (*CE*–*V*) curves (**f**) of green PeLEDs written on the pristine paper substrate and the PDMS-coated paper substrate. The inset in **e** shows the EL image of a handwritten $MAPbBr_3$ green LED. Scale bar, 500 µm. **g**,**h**, Characterization of the *J*–*V* and *L*–*V* curves (**g**) and the *CE*–*V* curves (**h**) of red and blue PeLEDs written on the PDMS-coated paper substrate. The insets in **g** show EL images of the handwritten $BA_2(MAPbI_3)_{n-1}PbI_4$-based red PeLED (left) and the $MAPb(Cl/Br)_3$-based blue PeLED (right). Scale bars, 500 µm. **i**, Normalized luminance and current efficiency of the $MAPbBr_3$ green PeLED measured after 5,000 bending cycles with a curvature radius of 1 mm. The insets show the experimental setup for the bending tests at relaxed and bent states. Scale bar, 1 cm.

were observed under illumination. The existence of a V_{oc} can be attributed to the parasitic photovoltaic effect from the asymmetric bottom electrodes, specifically parasitic Schottky junctions at the interface between the electrodes and the perovskite. Therefore, the photoconductor configuration can also function without a bias voltage. Curves of the responsivity (R) and the photocurrent ($I_{ph} = I_{light}$-I_{dark}) against the light intensity (I_v) under different bias voltages were examined, as shown in Supplementary Fig. 13.

The dynamic photoresponses of the vertical and lateral PePDs are plotted in Fig. 5c,f, indicating a repeatable and monotonically increasing photoresponse with an increasing light intensity. For the vertical photodiode, the rise/fall time (t_{rise}/t_{fall}) should be much shorter than the measured 15 ms, which was due to the limitations of our semiconductor analyser's sampling rate, whereas for the lateral photoconductor, t_{rise} was around 100 ms and t_{fall} was less than 15 ms (Supplementary Fig. 13). Absorption spectra confirmed that the selection of the polymer additive (none, PMMA or PS) had little influence on the intrinsic light-absorbing properties (Supplementary Fig. 14). To verify the hypothesis that the perovskite/PMMA composite is the optimal choice for PD applications, we tested additional photodiodes using the $MAPbBr_3$/PS composite as the photoactive layer (Supplementary Fig. 15 and Table 5). Furthermore, handwritten PePDs enable easy customization of the spectral response by modifying the perovskite's bandgap and absorption spectrum (Supplementary Fig. 16).

Conclusion

Our handwriting fabrication and toolkit (ballpoint pens and formulated inks) have successfully broken the limitations of conventional substrates for perovskite optoelectronic devices and enable the fabrication of devices on unconventional substrates such as paper, textiles, plastics, elastomers and rubber. The self-planarization effect of the PEO component in the PEDOT:PSS/PEO blend enables devices to be drawn directly on unmodified pristine paper. The direct handwriting method also provides controllability for the patterning of conformal optoelectronic devices on non-planar and deformable surfaces. Our formulated inks offer great versatility for building various optoelectronic devices with different configurations in a mask-free, on-demand, energy-saving and ultrafast manner, enabling high-performance devices to be manufactured within minutes, even by untrained individuals. Overall, such a user- and eco-friendly handwriting approach

https://doi.org/10.1038/s41566-023-01266-1

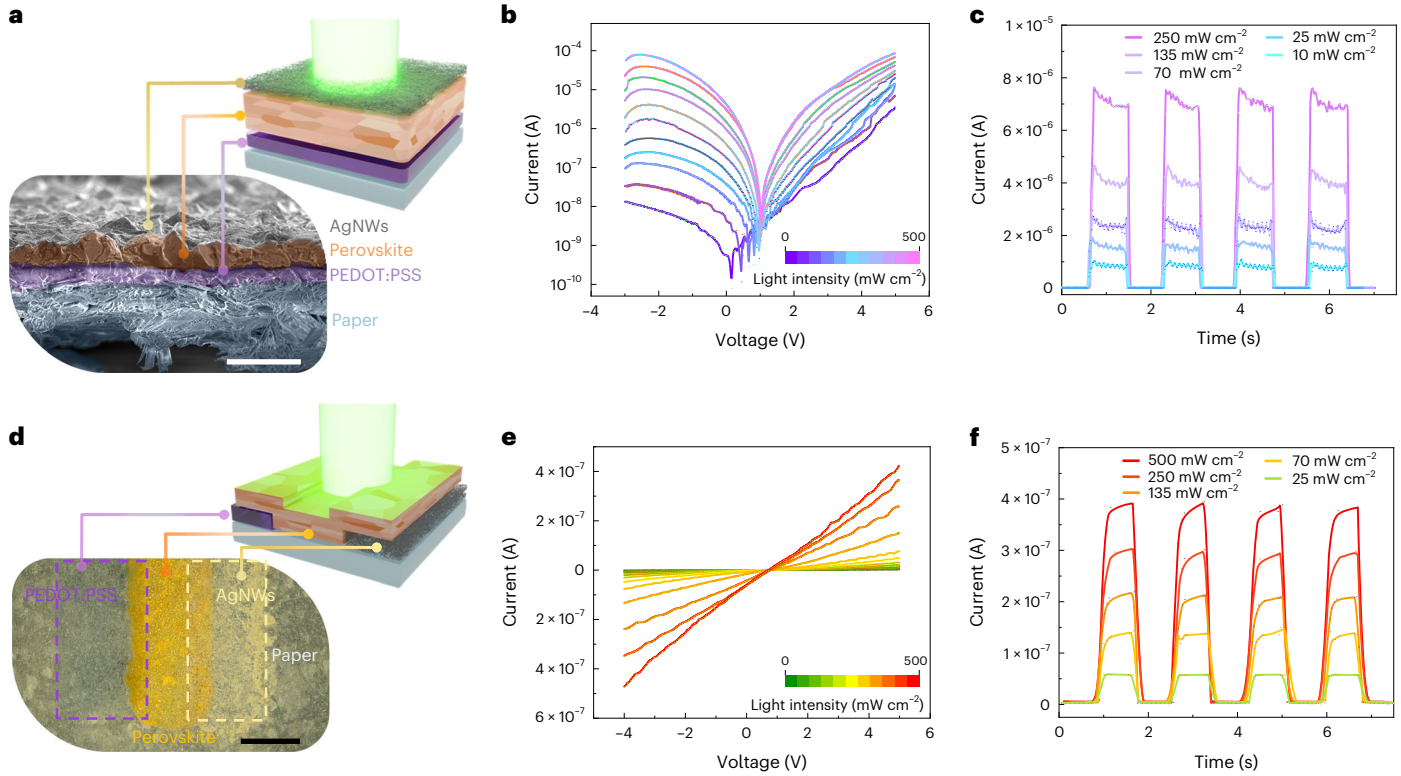

Fig. 5 | Performance characterization of the handwritten PePDs on paper. **a**,**d**, Schematics of handwritten PePDs with the vertical photodiode configuration (**a**) and lateral photoconductor configuration (**d**) under 532 nm light illumination. The inset in **a** shows the corresponding cross-sectional SEM image of the vertical photodiode configuration. The inset in **d** shows the corresponding top-view optical microscopy image of the lateral photoconductor configuration. Scale bars, 10 μm (**a**) and 500 μm (**d**). **b**,**e**, Characterization of the current–voltage (*I*–*V*) curves under dark conditions and with the incident light intensity varying from 0.1 to 500 mW cm^{-2} for the vertical photodiode (**b**) and the lateral photoconductor (**e**). **c**,**f**, Dynamic photoresponse measured under different light intensities and at a bias voltage of −0.5 V for the vertical photodiode (**c**) and −4.0 V for the lateral photoconductor (**f**).

could contribute to multiple application scenarios, for example, in early-stage product demonstration, science popularization and educational purposes. Handwriting could potentially benefit from the use of non-toxic lead-free perovskites as promising candidates for the construction of low-cost and lightweight paper- or textile-based LEDs and PDs, which could serve as a pragmatic means to integrate optoelectronic modules into wearable electronics and disposable biomedical sensors.

Online content

Any methods, additional references, Nature Portfolio reporting summaries, source data, extended data, supplementary information, acknowledgements, peer review information; details of author contributions and competing interests; and statements of data and code availability are available at https://doi.org/10.1038/s41566-023-01266-1.

References

1. Liang, J., Li, L., Niu, X., Yu, Z. & Pei, Q. Elastomeric polymer light-emitting devices and displays. *Nat. Photonics* **7**, 817–824 (2013).
2. Yu, Z., Niu, X., Liu, Z. & Pei, Q. Intrinsically stretchable polymer light-emitting devices using carbon nanotube–polymer composite electrodes. *Adv. Mater.* **23**, 3989–3994 (2011).
3. Lien, D.-H. et al. Large-area and bright pulsed electroluminescence in monolayer semiconductors. *Nat. Commun.* **9**, 1229 (2018).
4. Wang, C. et al. User-interactive electronic skin for instantaneous pressure visualization. *Nat. Mater.* **12**, 899–904 (2013).
5. Chou, S. Y. et al. Transparent perovskite light-emitting touch-responsive device. *ACS Nano* **11**, 11368–11375 (2017).
6. Gu, L. et al. A biomimetic eye with a hemispherical perovskite nanowire array retina. *Nature* **581**, 278–282 (2020).
7. Gu, L. et al. 3D arrays of 1024-pixel image sensors based on lead halide perovskite nanowires. *Adv. Mater.* **28**, 9713–9721 (2016).
8. Rao, Z. et al. Curvy, shape-adaptive imagers based on printed optoelectronic pixels with a kirigami design. *Nat. Electron.* **4**, 513–521 (2021).
9. Ershad, F. et al. Ultra-conformal drawn-on-skin electronics for multifunctional motion artifact-free sensing and point-of-care treatment. *Nat. Commun.* **11**, 3823 (2020).
10. Lin, K. et al. Perovskite light-emitting diodes with external quantum efficiency exceeding 20 per cent. *Nature* **562**, 245–248 (2018).
11. Wang, N. N. et al. Perovskite light-emitting diodes based on solution-processed self-organized multiple quantum wells. *Nat. Photonics* **10**, 699–704 (2016).
12. Bade, S. G. et al. Fully printed halide perovskite light-emitting diodes with silver nanowire electrodes. *ACS Nano* **10**, 1795–1801 (2016).
13. Kim, Y. H. et al. Exploiting the full advantages of colloidal perovskite nanocrystals for large-area efficient light-emitting diodes. *Nat. Nanotechnol.* **17**, 590–597 (2022).
14. Zhu, M. et al. Electrohydrodynamically printed high-resolution full-color hybrid perovskites. *Adv. Funct. Mater.* **29**, 1903294 (2019).
15. Zhao, J. et al. High-speed fabrication of all-inkjet-printed organometallic halide perovskite light-emitting diodes on elastic substrates. *Adv. Mater.* **33**, 2102095 (2021).
16. Tsai, H. et al. Bright and stable light-emitting diodes made with perovskite nanocrystals stabilized in metal–organic frameworks. *Nat. Photonics* **15**, 843–849 (2021).

17. Tian, Y. et al. Highly efficient spectrally stable red perovskite light-emitting diodes. *Adv. Mater.* **30**, 1707093 (2018).
18. Fang, Y. J., Dong, Q. F., Shao, Y. C., Yuan, Y. B. & Huang, J. S. Highly narrowband perovskite single-crystal photodetectors enabled by surface-charge recombination. *Nat. Photonics* **9**, 679–686 (2015).
19. Swarnkar, A. et al. Quantum dot-induced phase stabilization of α-$CsPbI_3$ perovskite for high-efficiency photovoltaics. *Science* **354**, 92–95 (2016).
20. Lei, Y. et al. A fabrication process for flexible single-crystal perovskite devices. *Nature* **583**, 790–795 (2020).
21. Seo, H. K. et al. Efficient flexible organic/inorganic hybrid perovskite light-emitting diodes based on graphene anode. *Adv. Mater.* **29**, 1605587 (2017).
22. Kim, T. H. et al. Full-colour quantum dot displays fabricated by transfer printing. *Nat. Photonics* **5**, 176–182 (2011).
23. Pan, T., Liu, S., Zhang, L., Xie, W. & Yu, C. A flexible, multifunctional, optoelectronic anticounterfeiting device from high-performance organic light-emitting paper. *Light Sci. Appl.* **11**, 59 (2022).
24. Zhu, H. L. et al. Biodegradable transparent substrates for flexible organic-light-emitting diodes. *Energy Environ. Sci.* **6**, 2105–2111 (2013).
25. Gao, L. et al. Flexible, transparent nanocellulose paper-based perovskite solar cells. *npj Flex. Electron.* **3**, 4 (2019).
26. Yoon, D. Y. & Moon, D. G. Bright flexible organic light-emitting devices on copy paper substrates. *Curr. Appl. Phys.* **12**, e29–e32 (2012).
27. Choi, S. et al. Multi-directionally wrinkle-able textile OLEDs for clothing-type displays. *npj Flex. Electron.* **4**, 33 (2020).
28. Kim, H., Kwon, S., Choi, S. & Choi, K. C. Solution-processed bottom-emitting polymer light-emitting diodes on a textile substrate towards a wearable display. *J. Inf. Disp.* **16**, 179–184 (2015).
29. Shi, X. et al. Large-area display textiles integrated with functional systems. *Nature* **591**, 240–245 (2021).
30. Dai, X. et al. Solution-processed, high-performance light-emitting diodes based on quantum dots. *Nature* **515**, 96–99 (2014).
31. Chen, J. et al. Efficient and bright white light-emitting diodes based on single-layer heterophase halide perovskites. *Nat. Photonics* **15**, 238–244 (2021).
32. Lei, Y. et al. Controlled homoepitaxial growth of hybrid perovskites. *Adv. Mater.* **30**, 1705992 (2018).
33. Xing, G. et al. Low-temperature solution-processed wavelength-tunable perovskites for lasing. *Nat. Mater.* **13**, 476–480 (2014).
34. Chen, X. M. et al. Solution-processed inorganic perovskite crystals as achromatic quarter-wave plates. *Nat. Photonics* **15**, 813–816 (2021).
35. Bade, S. G. R. et al. Stretchable light-emitting diodes with organometal-halide-perovskite–polymer composite emitters. *Adv. Mater.* **29**, 1607053 (2017).
36. Zhou, Y. et al. A universal method to produce low-work function electrodes for organic electronics. *Science* **336**, 327–332 (2012).

Methods

Materials

Lead(II) bromide ($PbBr_2$; 99.999%), lead(II) iodide (PbI_2; 99.999%), lead(II) chloride ($PbCl_2$; 99.999%), PEO (average $M_v \approx 5{,}000{,}000$), PS (average $M_w \approx 192{,}000$), *N*,*N*-dimethylformamide (DMF; 99.8%), dimethyl sulfoxide (DMSO; >99.9%), toluene (anhydrous, 99.8%), branched PEI (average $M_w \approx 25{,}000$ by light scattering, average $M_n \approx 10{,}000$ by gel permeation chromatography), Triton X-100, ethylene glycol and PEDOT:PSS (1.1% in H_2O) were purchased from Sigma-Aldrich. 4-Methyl-2-pentanone (99%) was purchased from Alfa Aesar. PMMA ($M_w \approx 950{,}000$) was purchased from MicroChem. Methylammonium bromide (MABr), methylammonium iodide (MAI) and methylammonium chloride (MACl) were purchased from 1-Material. The Sylgard 184 kit, including the silicone elastomer base and curing agent, was purchased from Dow. The AgNW dispersion (in isopropyl alcohol (IPA); diameter: ~90 nm, length: 20–30 μm) was purchased from ACS Material.

Synthesis of perovskites

$MAPbBr_3$ for green-coloured PeLEDs was synthesized following the same process as reported previously[15]. To obtain $MAPb(Cl_{1-x}Br_x)_3$ and $MAPb(Br_xI_{1-x})_3$ for multicolour PeLEDs, pure $MAPbX_3$ (X = Cl, Br or I) perovskites were first prepared by mixing the PbX_2 salt and MAX precursor at a molar ratio of 1:2, followed by dissolving the mixture in anhydrous DMSO to reach a concentration of 1 M. The suspension was stirred at 80 °C to obtain a transparent solution without any sediment. The hybrid perovskite $MAPb(Cl_{1-x}Br_x)_3$ or $MAPb(Br_xI_{1-x})_3$ was then obtained by mixing pure $MAPbBr_3$ and $MAPbCl_3$ or $MAPbBr_3$ and $MAPbI_3$, respectively, at the desired molar ratios. To expedite halide-anion substitution, the mixed solution needs to be stirred at 80 °C, which is also necessary to obtain a stable and homogeneous ink for further use. The quasi-2D $BA_2(MAPbI_3)_{n-1}PbI_4$ perovskite for red-coloured PeLEDs was prepared by dissolving the organic salt *n*-butylammonium iodide (BAI) in anhydrous DMSO to reach a concentration of 0.5 M followed by stirring at 80 °C. The BAI solution was then added to the as-prepared $MAPbI_3$ at the desired ratio and stirred to obtain the homogeneous quasi-2D RPP ink.

Preparation and characterization of substrates

The oil-treated semi-transparent paper substrate was achieved by putting a few oil droplets onto the paper substrate, followed by spreading the oil uniformly using a glass slide and wiping away any excess. Because the refractive index of oil ($n = 1.466–1.474$) is much closer to that of cellulose fibres ($n = 1.469$) than it is to air ($n = 1.000$), less light will be scattered or refracted when interacting with the oil-smeared paper, allowing more light to be transmitted through the cellulose fibres and making the paper more transparent. To prepare the PDMS-coated paper substrate, the PDMS solution was first prepared by mixing the elastomer base and curing agent from the Sylgard 184 kit at a weight ratio of 10:1, followed by dilution using the 4-methyl-2-pentanone organic solvent and stirring at 500 revolutions per minute to obtain a less viscous mixture. A few liquid PDMS droplets were then pipetted onto the pristine paper substrate followed by blade coating until a very thin and uniform PDMS layer was formed on the paper. The paper was then annealed in an oven for solvent evaporation and curing of the PDMS. The textile substrates used in this work (cotton, voile, chiffon and organza) were all common fabrics found in daily life. The fabrics were prepared following the same PDMS-coating process until all voids between the woven fibres were filled. The fabrics were then annealed in an oven until the PDMS was fully cured. The rest of the substrates used in the work, including vinyl gloves, polyethylene terephthalate, the glass vial and rubber balloon, were all found in daily life and were used without further surface treatment, except for wettability modification via oxygen-plasma treatment if necessary.

Ink formulations

The PEDOT:PSS/PEO composite ink was prepared following the method reported in our previous work[37]. In brief, a viscous PEO solution (10 mg ml^{-1}) was prepared by dissolving PEO powder in DMF with stirring at 60 °C. Then the PEDOT:PSS/PEO composite ink was obtained by mixing the PEDOT:PSS ink with the PEO solution at the desired weight ratio. The perovskite/PEO composite ink was prepared by mixing the as-prepared perovskite ink and PEO viscous solution at a 2:1 weight ratio. The perovskite/PS and perovskite/PMMA composite inks were prepared similarly by mixing the as-prepared perovskite ink and PS or PMMA solutions (where the PS solution (10 mg ml^{-1}) was prepared by dissolving PS pellets into toluene, and the PMMA solution (10 mg ml^{-1}) was prepared by diluting PMMA with DMF) at a 2:1 weight ratio. The PEI ink (20 mg ml^{-1}) was prepared by dissolving PEI in IPA with stirring. Low-boiling-point solvents such as toluene and IPA were used in these inks to expedite or eliminate the annealing process, and the samples were allowed to dry naturally at room temperature. Finally, the AgNW ink was formulated by adding ethylene glycol (20 vol%) to the as-purchased AgNW dispersion with sonication for 60 s before use to eliminate the aggregation of entangled nanowires.

Ballpoint pen preparation

Commercial ballpoint pens were used, and the refills were disassembled by disconnecting the tips from the ink cartridges. The tips and cartridges were cleaned thoroughly using IPA and acetone, followed by blow drying using compressed air. The formulated inks were then injected into the empty cartridges, using syringes, for future use.

Fabrication of PeLEDs and PePDs

To fabricate the PeLEDs on pristine paper, the PEDOT:PSS/PEO composite ink was first handwritten onto the paper surface following the user's normal way of handwriting, and the paper substrate was annealed either in an oven or on a hotplate until the solvent was fully evaporated. Next, the perovskite/polymer composite inks of various colours were handwritten directly on top of the PEDOT:PSS/PEO film, followed by annealing of the sample. Then, the PEI ink was handwritten gently on top of the perovskite layer. Finally, as a last step, the AgNW ink was written gently on top of the PEI buffer, leaving behind an AgNW network that uniformly covers the desired active region. The use of IPA solvent with a low boiling point in both the PEI and AgNW inks enables the annealing processes for these layers to be skipped, which helps to shorten the fabrication time substantially. Similar to handwritten preparation of PeLEDs on paper substrates, the process for writing the PeLEDs on PDMS-treated paper/textile, glass, plastic, rubber or metal substrates was largely the same as above, except that the substrates were first treated using oxygen plasma to render the surface hydrophilic and improve the wetting of the ink.

The fabrication process for PePDs with a vertical configuration was very similar to that for PeLED fabrication described above, except that the as-purchased AgNW ink was used, to reduce the erosion effects on the perovskite layer underneath. To fabricate PePDs with a lateral configuration, a pair of parallel electrodes were first handwritten on pristine paper using the PEDOT:PSS/PEO and AgNW inks, respectively. The gap between these two electrodes determines the channel length of the PePD and can be carefully customized using a ruler and ballpoint pens with fine nibs. A channel length as narrow as tens of micrometres was achieved. Next, the perovskite/polymer composite ink was written to bridge the two bottom electrodes.

Characterization of PeLEDs and PePDs

The PL spectra and absorption spectra of the perovskite materials were characterized using an RF-6000 fluorometer (Shimadzu) and a Lambda 950 UV/vis/NIR spectrophotometer (Perkin-Elmer), respectively. The

transmittance spectra of the different substrates were characterized with a Varian Cary 50 Bio spectrophotometer. The SEM images were obtained using a Quattro ESEM system (Thermofisher). The luminance–voltage (L–V) curves of the PeLED were characterized using a calibrated silicon photodiode that can capture the light emitted from the PeLEDs inside a dark box. A semiconductor device analyser (B1500A, Keysight) was used to apply bias voltages and measure the PeLED device current and the PePD dark and light current. Bending tests were carried out using an automatic syringe pump (Legato 110, KD Scientific), whose motion, such as the moving speed and repeating cycles, can be programmed precisely. All PePD measurements were carried out inside a probe station using the semiconductor device analyser and a custom-made tunable laser irradiation system with a 532 nm green laser, a light chopper and a power supply. The power intensity of the laser was calibrated using a digital optical power and energy meter (PM100D, Thorlabs) with a photodiode power sensor (S121C, Thorlabs). The transient photoresponse was characterized using the semiconductor analyser in current–time (I–t) sweeping mode with a fixed bias voltage. Note that the rise/fall times of the PePD were limited by the sampling rate of the equipment. The responsivity of the PePD is defined as $R = I_{ph}/(I_v \cdot A)$, where I_v and A represent the light intensity and active area, respectively.

Data availability

All data supporting the results in this study are provided in the Article and Supplementary Information. Additional data are available from the corresponding authors upon reasonable request.

References

37. Lo, L. W. et al. An inkjet-printed PEDOT:PSS-based stretchable conductor for wearable health monitoring device applications. *ACS Appl. Mater. Interfaces* **13**, 21693–21702 (2021).

Acknowledgements

This work was partially funded by the Bill & Melinda Gates Foundation under award numbers INV-005417 and INV-035476 (J.Z., L.-W.L. and C.W.) and Washington University. We also acknowledge the Institute of Materials Science and Engineering at Washington University for the use of instruments and staff assistance.

Author contributions

J.Z. and C.W. conceived the idea and designed the experiments. J.Z. carried out all the experiments including the ink development, device fabrication, characterization of the materials and device measurements. L.-W.L. contributed to part of the ink formulation and development of the printing process. J.Z., Z.Y., and C.W. performed the data analysis. J.Z. and C.W. wrote the paper while all authors provided feedback.

Competing interests

The authors declare no competing interests.

Additional information

Supplementary information The online version contains supplementary material available at https://doi.org/10.1038/s41566-023-01266-1.

Correspondence and requests for materials should be addressed to Zhibin Yu or Chuan Wang.

Peer review information *Nature Photonics* thanks Qibing Pei, Sheng Xu, Cunjiang Yu and the other, anonymous, reviewer(s) for their contribution to the peer review of this work.